of change. It also should be noted that, at any stage during the film formation, the imaginary part of the optical constant, k_f, does not have a near-zero value which might be associated with an electronically insulating property of the anodic film. Such was the case with the passive films on iron and nickel as reported previously.[16-18] These transient behaviors, therefore, seem to be a general trend among passive films on metals such as iron, nickel, and cobalt.

Summary

By means of transient recordings of the three-parameter ellipsometry measurements, the thickness and the optical constants of passive film forming on cobalt under potentiostatic condition were determined as functions of time. The film-free reference surface of cobalt for the optical measurements was obtained by complete cathodic reduction of the surface film in the presence of EDTA. The growth of the passive film was mostly complete in 3-4 seconds from the onset of the passivating potential, and was followed by a slight decrease in the thickness in the time range of 4-40 s. The optical constants of the passive film showed gradual changes during the changes in the thickness. The thickness and the optical poperties at the steady state of passivation depended on the potential of the electrode. Form the coulometric and optical data, the composition of the passive films was deduced to be close to CoO at potentials lower than 0.15 V *vs.* SCE, to Co_2O_3 at higher potentials in the 0.25 to 0.35 V range, and to Co_3O_4 at intermediate potentials. It is concluded that the passive films undergo a gradual change during the passivation instead of a phase-transition type of change, since no abrupt change in the optical constants of the passive film was observed.

Acknowledgement. Financial support for this work from the Korea Science and Engineering Foundation is gratefully acknowledged. Dr. Duckhwan Lee assisted in modifying the computer program used in the calculation.

References

1. C. A. Melendres and S. Xu, *J. Electrochem. Soc.*, **131**, 2239 (1984).
2. G. W. Simmons, E. Kellerman, and H. Leidheiser Jr., *ibid.*, **123**, 1276 (1976).
3. J. Chon and W. Paik, *J. Korean Chem. Soc.*, **18**, 391 (1974).
4. T. Ohtsuka and N. Sato, *J. Jpn. Inst. Met.*, **39**, 60 (1975).
5. T. Ohtsuka, K. Kudo, and N. Sato, *ibid*, **40**, 124 (1976).
6. N. Sato and T. Ohtsuka, *J. Electrochem. Soc.*, **125**, 1735 (1978).
7. N. Sato and T. Ohtsuka, *ibid*, **128**, 2522 (1981).
8. W. Paik and J. O'M. Bockris, *Surface Sci.*, **28**, 61 (1971).
9. S. H. Kim, W. Paik, and J. O'M. Bockris, *ibid.*, **33**, 617 (1972).
10. S. Gottesfeld and B. Reichman, *ibid*, **44**, 377 (1974).
11. J. Horkans, B. D. Cahan, and E. Yeager, *ibid*, **46**, 1 (1974).
12. S. Gottesfeld, M. Babai, and B. Reichman, *ibid*, **56**, 355 (1976).
13. W. Paik and Z. Szklarska-Smialowska, *ibid*, **96**, 401 (1980).
14. W. Paik, in: "*Electrochmistry*", *International Review of Science, Physical Chemistry Series One, Vol. 6*, J. O'M. Bockris ed., Butterworth, 1973.
15. B. Park, W. Paik, and I. Yeo, *J. Korean Chem. Soc.*, **22**, 365 (1978).
16. D. Kim and W. Paik, *ibid.*, **26**, 369 (1982).
17. I. Yeo and W. Paik, *ibid.*, **28**, 271 (1984).
18. Y. Kang and W. Paik, Surface Sci., **182**, 259 (1987).
19. Z. Szklarska-Smialowska, T. Zakroczymski, and C. J. Fan, *J. Electrochem. Soc.*, **132**, 2543 (1985).
20. T. Zakroczymski, Z. Szklarska-Smialowska, *ibid.*, **132**, 2548 (1985).
21. *American Institute of Physics Handbook*, 3rd ed., 1972.
22. R. J. Powell and W. E. Spicer, *J. Phys. Review B*, **2**, 2182 (1970).
23. J. G. Cook and G. C. Aers, *Surface Sci.*, **166**, 333 (1986).
24. K. J. Boyle, E. G. King, and K. C. Conway, *J. Am. Chem. Soc.*, **76**, 3835 (1954).
25. H. Göhr, Electrochim. Acta, **11**, 827 (1966).

The Analytical Solutions for Finite Clusters of Cubic Lattices

Gean-Ha Ryu and Hojing Kim*

Department of Chemistry, Seoul National University, Seoul 151-742. *Received June 15, 1991*

Using the Hückel method, we obtain the analytical expressions for eigenvalues and eigenvectors of s.c., f.c.c. and b.c.c. clusters of rectangular parallelepiped shape, and of an arbitrary size. Our formulae converage to those derived from the Bloch sum, in the limit of infinite extension. DOS and LDOS reveal that the major contribution of the states near Fermi level originates from the surface atoms, also symmetry of DOS curves disappears by the introduction of 2nd nearest neighbor interactions, in all the cubic lattices. An accumulation of the negative charges on surface of cluster is observed.

Introduction

There are two major approaches in explaining the properties of solid. One is solid state physics in which a solid is regarded as a set of atoms or molecules of a large number, which is considered to have translational symmetry. The

other is MO theory in chemistry, in which a solid is treated as a large molecule. Of the two, MO theory is preferable for investigating the surface phenomena (catalysis, corrision, SERS, etc.), for which are recognized as the local properties on surface rather than as the bulk.

In MO theory, there are several computational tools to elucidate adsorbate-substrate interaction: extended Hückel[1-3], CNDO[4], pseudo-potential techniques[5], Xα theory[6,7], and *ab intio* Hatree-Fock method[8-10] etc. It is difficult to describe the metal clusters of a practical size since accuracy costs much computaional efforts.

There have been some efforts to obtain analytical solutions of the clusters of an arbitrary size. Messmer[11] obtained an analytical solution of simple cubic (s.c.) cluster within the framework of Hückel theory, with only the nearest neighbor interaction being taken into account. Identifying the s.c. cluster as the two interpenetrated face centered cubic (f.c.c.) clusters, Bilek and Kadura[12] obtained the expressions for the energy and the wave function of f.c.c. cluster. They treated only the 1st nearest neighbor interactions and assumed one *s*-atomic orbital per site for basis. Employing Bloch sum, Slater and Koster[13] derived the energy expressions for the infinite crystals. With some modification of this results of infinite crystals, Salem[14] derived the solution of s.c. and f.c.c. cluster of a finite size, taking only 1st nearest neighbor interactions into account. He discussed the mixing among cluster functions of a *s*-type and five *d*-types with the same wave vectors, and also the mixing among states of different wave vectors. He also discussed the interaction between H_2 molecule and Ni cluster with the cluster functions[14,15].

In present work, Messmer's work is extended to 3rd nearest neighbor interactions. Recognizing that f.c.c. and body centered cubic (b.c.c.) lattices are substructures of s.c., we derive the analytic Hückel solutions of these clusters. In other words, a s.c. cluster can be partitioned into two f.c.c. subclusters or four b.c.c. subclusters. If only the nearest neighbor interactions are taken into account for s.c. cluster, then there results Messmer's solution of s.c. cluster. If one regards only 2nd nearest neighbor interactions in s.c. cluster being nonzero, then the derived solution is the Hückel one of two non-interacting f.c.c. subclusters with only 1st nearest neighbor interactions. Again, if 1st and 2nd nearest neighbor interactions are ignored, the resulting Hückel solution is the one for the four non-interacting b.c.c. subclusters.

These results are compared with those of infinite solid that can be obtained with the same oder of neighbor interactions. It is found that in f.c.c. and b.c.c. clusters with the interactions up to 2nd nearest neighbor (4th in s.c.), the energy expressions have the extra term which does not appear in those of infinite crystals. The extra term originates from the existence of surface of the finite clusters. Density of states (DOS) and local density of states (LDOS) are also computed. The charge density at the several representative points of the clusters, the variation of charge distribution *vs.* the size of a cluster and the characters of each lattices are discussed.

Theory

Let us consider s.c. cluster of rectangular parallelepiped, made of N_A, N_B, and N_C atoms in *x*, *y*, and *z* directions,

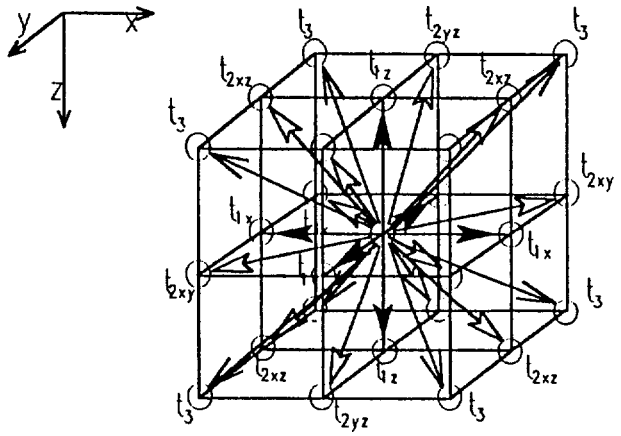

Figure 1. The interaction up to 3rd nearest neighbors. For example, t_{1x} and t_{2xy} represent 1st nearest neighbor interaction along *x*-direction and 2nd one in *xy*-plane, respectively.

respectively. One atomic orbital χ (*s*, *p* or *d* orbitals) per lattice point is chosen as basis. If the interactions up to 3rd nearest neighbor are considered, the elements of Hamiltonian matrix of this cluster can be written as follows:

$$\langle\chi_\mu|\hat{H}|\chi_\mu\rangle=\varepsilon_0 \tag{1}$$

$$\langle\chi_\mu|\hat{H}|\chi_\nu\rangle=\begin{cases} t_{1x} \text{ (if } \mu \text{ and } \nu \text{ are 1st nearest neighbors along } x\text{-axis)} \\ t_{1y} \text{ (if } \mu \text{ and } \nu \text{ are 1st nearest neighbors along } y\text{-axis)} \\ t_{1z} \text{ (if } \mu \text{ and } \nu \text{ are 1st nearest neighbors along } z\text{-axis)} \\ t_{2xy} \text{ (if } \mu \text{ and } \nu \text{ are 2nd nearest neighbors in } xy\text{-plane)} \\ t_{2yz} \text{ (if } \mu \text{ and } \nu \text{ are 2nd nearest neighbors in } yz\text{-plane)} \\ t_{2xz} \text{ (if } \mu \text{ and } \nu \text{ are 2nd nearest neighbors in } xz\text{-plane)} \\ t_3 \text{ (if } \mu \text{ and } \nu \text{ are 3rd nearest neighbors)} \\ 0 \text{ (otherwise).} \end{cases} \tag{2}$$

The subscripts μ and ν represent the sites of atoms in cluster. Being tight-binding approximation, the overlap integral is neglected *i.e.*

$$\langle\chi_\mu|\chi_\nu\rangle=\delta_{\mu\nu}. \tag{3}$$

The secular equation is

$$\boldsymbol{H}\boldsymbol{D}=\boldsymbol{D}\boldsymbol{\varepsilon} \tag{4}$$

where the dimension of each matrix is $N_AN_BN_C\times N_AN_BN_C$. The elements of the matrix $\boldsymbol{H}$ are given in Eqs. (1) and (2), and the matrix ε is diagonal and contains the eigenvalues. The matrix $\boldsymbol{D}$ is the eigenvector matrix which is made of coefficients $d_{\alpha\beta}$ of molecular orbitals such that

$$\Psi_\beta=\sum_\alpha \chi_\alpha d_{\alpha\beta} \qquad \alpha,\ \beta=1,\ 2,\ \cdots\ N_AN_BN_C. \tag{5}$$

Then the eigenvalues are obtained by solving

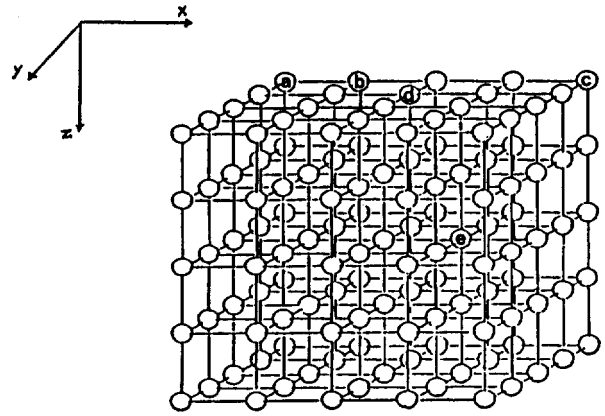

Figure 2. Indexing methods of atoms in 5×5×5 s.c. cluster. In *p*-indexing method, *a*, *b*, *c*, *d* and *e* are (1, 1, 1), (2, 1, 1), (5, 1, 1), (3, 2, 1) and (4, 3, 3), respectively. In α-indexing method, these are 1, 2, 5, 8 and 64, respectively.

$$|H-\varepsilon\,\mathbf{1}| \equiv |C| = 0. \tag{6}$$

For describing the position of an atom in cluster, the position vector $\vec{p}$ and sequential index α which corresponds to vector $\vec{p}$ are used. That is,

$$\vec{p} = (i,\ j,\ k) \tag{7}$$

$$\alpha = (k-1)\,N_B N_A + (j-1)\,N_A + i \tag{8}$$

where $i=1, 2, 3, \cdots N_A$, $j=1, 2, 3, \cdots N_B$, $k=1, 2, 3, \cdots N_C$. Figure 2 represents the method describing the position vector $\vec{p}$ and the index α in 5×5×5 s.c. cluster. Throughout this article, two index systems are used together as occasion demands.

Using sequential index α, matrix C of Eq. (6) is given in a block form:

$$C = \begin{bmatrix} B_1 & B_2 & O_B & O_B & \cdots\cdots \\ B_2 & B_1 & B_2 & O_B & \cdots\cdots \\ O_B & B_2 & B_1 & B_2 & \cdots\cdots \\ \vdots & \vdots & \vdots & \vdots & \\ \vdots & \vdots & \vdots & \vdots & \end{bmatrix} \tag{9}$$

which is $N_C \times N_C$ matrix whose elements themselves are matrices of dimension $N_A N_B \times N_A N_B$. Matrix O_B is null matrix and matrix B_1 and B_2 are written

$$B_1 = \begin{bmatrix} A_1 & A_2 & O_A & O_A & \cdots\cdots \\ A_2 & A_1 & A_2 & O_A & \cdots\cdots \\ O_A & A_2 & A_1 & A_2 & \cdots\cdots \\ \vdots & \vdots & \vdots & \vdots & \\ \vdots & \vdots & \vdots & \vdots & \end{bmatrix} \tag{10}$$

$$B_2 = \begin{bmatrix} A_3 & A_4 & O_A & O_A & \cdots\cdots \\ A_4 & A_3 & A_4 & O_A & \cdots\cdots \\ O_A & A_4 & A_3 & A_4 & \cdots\cdots \\ \vdots & \vdots & \vdots & \vdots & \\ \vdots & \vdots & \vdots & \vdots & \end{bmatrix} \tag{11}$$

respectively. All the matrices A_1, A_2, A_3, A_4 and O_A of Eqs. (10) and (11) themselves are the matrices of dimension $N_A \times N_A$, and O_A is the null matrix. The matrices A_1, A_2, A_3 and A_4 are given by

$$A_1 = \begin{bmatrix} \varepsilon_0-\varepsilon & t_{1x} & 0 & 0 & \cdots\cdots \\ t_{1x} & \varepsilon_0-\varepsilon & t_{1x} & 0 & \cdots\cdots \\ 0 & t_{1x} & \varepsilon_0-\varepsilon & t_{1x} & \cdots\cdots \\ \vdots & \vdots & \vdots & \vdots & \\ \vdots & \vdots & \vdots & \vdots & \end{bmatrix} \tag{12}$$

$$A_2 = \begin{bmatrix} t_{1y} & t_{2xy} & 0 & 0 & \cdots\cdots \\ t_{2xy} & t_{1y} & t_{2xy} & 0 & \cdots\cdots \\ 0 & t_{2xy} & t_{1y} & t_{2xy} & \cdots\cdots \\ \vdots & \vdots & \vdots & \vdots & \\ \vdots & \vdots & \vdots & \vdots & \end{bmatrix} \tag{13}$$

$$A_3 = \begin{bmatrix} t_{1z} & t_{2xz} & 0 & 0 & \cdots\cdots \\ t_{2xz} & t_{1z} & t_{2xz} & 0 & \cdots\cdots \\ 0 & t_{2xz} & t_{1z} & t_{2xz} & \cdots\cdots \\ \vdots & \vdots & \vdots & \vdots & \\ \vdots & \vdots & \vdots & \vdots & \end{bmatrix} \tag{14}$$

$$A_4 = \begin{bmatrix} t_{2yz} & t_3 & 0 & 0 & \cdots\cdots \\ t_3 & t_{2yz} & t_3 & 0 & \cdots\cdots \\ 0 & t_3 & t_{2yz} & t_3 & \cdots\cdots \\ \vdots & \vdots & \vdots & \vdots & \\ \vdots & \vdots & \vdots & \vdots & \end{bmatrix} \tag{15}$$

respectively. Solving[16,17] the secular equation (Eq. (6)) for the matrix C we can obtain the eigenvalues and eigenvectors of the cluster.

The cluster functions are identified with the position vector $\vec{q} = (l,\ m,\ n)$ in the state space or serial index β defined by

$$\beta = (n-1)\,N_B N_A + (m-1)\,N_A + l \tag{16}$$

where $l=1, 2, \cdots, N_A$, $m=1, 2, \cdots, N_B$, $n=1, 2, \cdots, N_C$.

When the interactions up to 3rd nearest neighbor are included, the eigenvalues and the eigenvectors of s.c. cluster of an arbitrary size are

$$\begin{aligned} \varepsilon_\beta = \varepsilon_0 &+ 2\left(t_{1x}\cos\frac{l\pi}{N_A+1} + t_{1y}\cos\frac{m\pi}{N_B+1} + t_{1z}\cos\frac{n\pi}{N_C+1}\right) \\ &+ 4\left(t_{2xy}\cos\frac{l\pi}{N_A+1}\cos\frac{m\pi}{N_B+1} + t_{2yz}\cos\frac{m\pi}{N_B+1}\cos\frac{n\pi}{N_C+1}\right. \\ &\left. + t_{2xz}\cos\frac{n\pi}{N_C+1}\cos\frac{l\pi}{N_A+1}\right) \\ &+ 8t_3\cos\frac{l\pi}{N_A+1}\cos\frac{m\pi}{N_B+1}\cos\frac{n\pi}{N_C+1} \end{aligned} \tag{17}$$

and

$$d_{\alpha\beta} = u_C(k,\ n)\ u_B(j,\ m)\ u_A(i,\ l) \tag{18}$$

where u_A, u_B, and u_C are

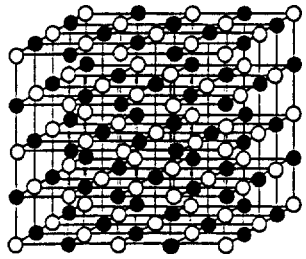

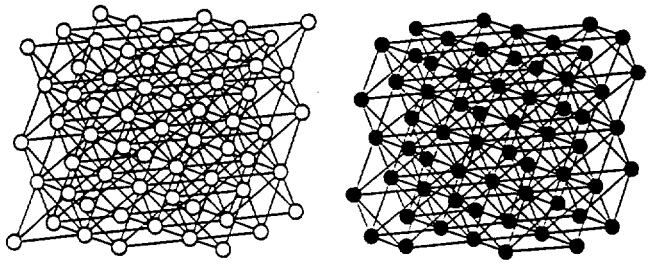

Figure 3. Two f.c.c. subclusters from parent s.c. cluster. If 1st and 3rd nearest neighbor interactions of s.c. cluster (a) are ignored, the two non-interacting f.c.c. subclusters (b) and (c) can be obtained. The solid lines of (b) and (c) connect 1st nearest neighbors in f.c.c. (*i.e.*, 2nd in s.c.).

$$u_A(i,\ l)=\left(\frac{2}{N_A+1}\right)^{1/2}\sin\left(\frac{il\pi}{N_A+1}\right) \tag{19}$$

$$u_B(j,\ m)=\left(\frac{2}{N_B+1}\right)^{1/2}\sin\left(\frac{jm\pi}{N_B+1}\right) \tag{20}$$

$$u_C(k,\ n)=\left(\frac{2}{N_C+1}\right)^{1/2}\sin\left(\frac{kn\pi}{N_C+1}\right). \tag{21}$$

Since an f.c.c. and a b.c.c. cluster are subclusters of s.c. cluster, we can derive the analytical solutions of these clusters. That is, assuming that the interactions between atoms which are 1st and 3rd nearest neighbors in parent s.c. cluster, are set to be zero ($t_{1x}=t_{1y}=t_{1z}=t_3=0$), then the s.c. cluster is divided into two non-interacting f.c.c. subcluster of interpenetrated form.

Using the same indexing system as defined above, we obtain the solutions which have two-fold degeneracy originated from two f.c.c. subclusters:

$$\beta_1 \longleftrightarrow q_1=(l,\ m,\ n) \tag{22}$$

$$\beta_2 \longleftrightarrow q_2=(N_A-l+1,\ N_B-m+1,\ N_C-n+1) \tag{23}$$

$$\varepsilon_{\beta_1}=\varepsilon_{\beta_2}=\varepsilon_0+4\left(t_{2xy}\cos\frac{l\pi}{N_A+1}\cos\frac{m\pi}{N_B+1}+t_{2yz}\cos\frac{m\pi}{N_B+1}\cos\frac{n\pi}{N_C+1}+t_{2xz}\cos\frac{n\pi}{N_C+1}\cos\frac{l\pi}{N_A+1}\right). \tag{24}$$

By simple trigonometric relation, the transformation of these two-fold degenerate eigenvectors can be made. Each of the transformed cluster orbitals has basis atomic orbitals centered exclusively on one of the two f.c.c. subclusters. That is

$$(d^{f_I}_{\alpha\beta_1}\ d^{f_{II}}_{\alpha\beta_2})=(d_{\alpha\beta_1}\ d_{\alpha\beta_2})\times\frac{1}{\sqrt{2}}\begin{bmatrix}1 & 1\\ 1 & -1\end{bmatrix} \tag{25}$$

where the superscripts f_I and f_{II} indicate the two subsclusters, respectively.

Accordingly, we may rewrite as

$$\varepsilon^{f_I}_{\beta_1}=\varepsilon^{f_{II}}_{\beta_2}=\varepsilon_0+4\left(t_{2xy}\cos\frac{l\pi}{N_A+1}\cos\frac{m\pi}{N_B+1}+t_{2yz}\cos\frac{m\pi}{N_B+1}\cos\frac{n\pi}{N_C+1}+t_{2xz}\cos\frac{n\pi}{N_C+1}\cos\frac{l\pi}{N_A+1}\right) \tag{26}$$

$$d^{f_I}_{\alpha\beta_1}=\frac{1}{\sqrt{2}}(d_{\alpha\beta_1}+d_{\alpha\beta_2})=\frac{1+(-1)^{i+j+k+1}}{\sqrt{2}}u_A(i,\ l)\,u_B(j,\ m)\,u_C(k,\ n) \tag{27}$$

$$d^{f_{II}}_{\alpha\beta_2}=\frac{1}{\sqrt{2}}(d_{\alpha\beta_1}-d_{\alpha\beta_2})=\frac{1-(-1)^{i+j+k-1}}{\sqrt{2}}u_A(i,\ l)\,u_B(j,\ m)\,u_C(k,\ n) \tag{28}$$

where $l=1,\ 2,\ \cdots,\ N_A$, $m=1,\ 2,\ \cdots,\ N_B$, $n=1,\ 2,\ \cdots,\ N_C$. And l, m, and n must satisfy the additional condition $\frac{l}{N_A+1}+\frac{m}{N_B+1}+\frac{n}{N_C+1}<\frac{3}{2}$.

Similarly, if 1st and 2nd nearest neighbor interactions of parent s.c. cluster are ignored ($t_{1x}=t_{1y}=t_{1z}=t_{2xy}=t_{2yz}=t_{2xz}=0$), there results four non-interacting b.c.c. subclusters. Representing the states with the index of parent s.c. cluster, it is clear that the four b.c.c. subclusters give four-fold degeneracy. That is, for q_1, q_2, q_3, and q_4 given as

$$\beta_1 \longleftrightarrow q_1=(l,\ m,\ n) \tag{29}$$

$$\beta_2 \longleftrightarrow q_2=(N_A-l+1,\ N_B-l+1,\ n) \tag{30}$$

$$\beta_3 \longleftrightarrow q_3=(N_A-l+1,\ m,\ N_C-n+1) \tag{31}$$

$$\beta_4 \longleftrightarrow q_4=(l,\ N_B-m+1,\ N_C-n+1) \tag{32}$$

the corresponding cluster orbitals Ψ_{β_1}, Ψ_{β_2}, Ψ_{β_3} and Ψ_{β_4} are degenerated

$$\varepsilon_{\beta_1}=\varepsilon_{\beta_2}=\varepsilon_{\beta_3}=\varepsilon_{\beta_4}=\varepsilon_0+8t_3\cos\frac{l\pi}{N_A+1}\cos\frac{m\pi}{N_B+1}\cos\frac{n\pi}{N_C+1}. \tag{33}$$

Through the transformation within the degenerate space, we can easily obtain the eigenvectors made of exclusively the atomic orbitals of each subcluster:

$$(d^{b_I}_{\alpha\beta_1}\ d^{b_{II}}_{\alpha\beta_2}\ d^{b_{III}}_{\alpha\beta_3}\ d^{b_{IV}}_{\alpha\beta_4})=(d_{\alpha\beta_1}\ d_{\alpha\beta_2}\ d_{\alpha\beta_3}\ d_{\alpha\beta_4})\times\frac{1}{2}\begin{bmatrix}1 & 1 & 1 & 1\\ 1 & -1 & -1 & 1\\ 1 & -1 & 1 & -1\\ 1 & -1 & -1 & 1\end{bmatrix} \tag{34}$$

where the superscripts b_I, b_{II}, b_{III} and b_{IV} indicatethe four b.c.c. subcluster.

More explicitly writing, we have:

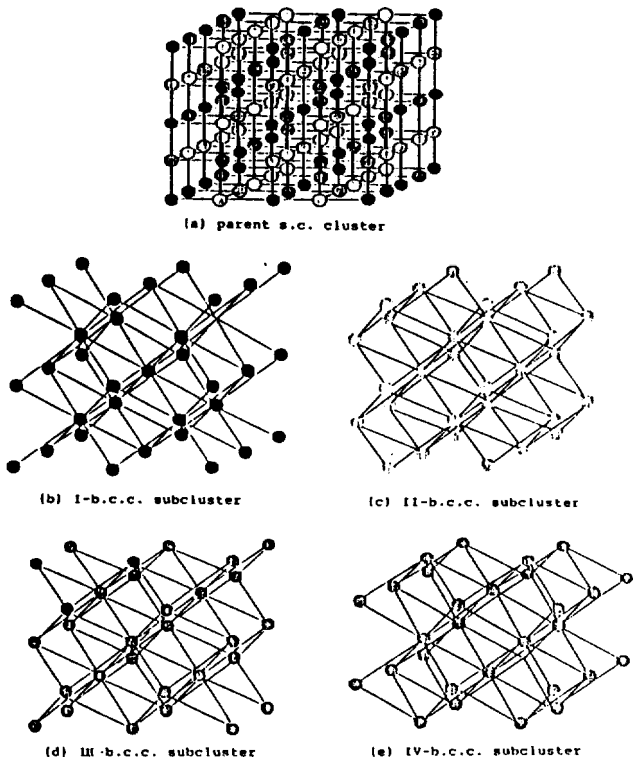

Figure 4. Four f.c.c. subclusters from parent s.c. cluster. If 1st and 2nd nearest neighbor interactions in parent s.c. cluster (a), are set to be zero, then the s.c. cluster is divided into four non-interacting b.c.c. subclusters (b), (c), (d) and (e). The solid lines of b.c.c. subclusters connect 1st nearest neighbors in b.c.c. (*i.e.*, 3nd in s.c.).

$$\varepsilon_{\beta_1}^{b_I}=\varepsilon_{\beta_2}^{b_{II}}=\varepsilon_{\beta_3}^{b_{III}}=\varepsilon_{\beta_4}^{b_{IV}}$$
$$=\varepsilon_0+8t_3\cos\frac{l\pi}{N_A+1}\cos\frac{m\pi}{N_B+1}\cos\frac{n\pi}{N_C+1} \quad (35)$$

$$d_{\alpha\beta_1}^{b_I}=\frac{1}{2}(d_{\alpha\beta_1}+d_{\alpha\beta_2}+d_{\alpha\beta_3}+d_{\alpha\beta_4})$$
$$=\frac{1+(-1)^{l+j}+(-1)^{l+k}+(-1)^{j+k}}{2}u_A(i,\ l)\,u_B(j,\ m)\,u_C(k,\ n) \quad (36)$$

$$d_{\alpha\beta_2}^{b_{II}}=\frac{1}{2}(d_{\alpha\beta_1}-d_{\alpha\beta_2}-d_{\alpha\beta_3}+d_{\alpha\beta_4})$$
$$=\frac{1-(-1)^{l+j}-(-1)^{l+k}+(-1)^{j+k}}{2}u_A(i,\ l)\,u_B(j,\ m)\,u_C(k,\ n) \quad (37)$$

$$d_{\alpha\beta_3}^{b_{III}}=\frac{1}{2}(d_{\alpha\beta_1}-d_{\alpha\beta_2}+d_{\alpha\beta_3}-d_{\alpha\beta_4})$$
$$=\frac{1-(-1)^{l+j}+(-1)^{l+k}-(-1)^{j+k}}{2}u_A(i,\ l)\,u_B(j,\ m)\,u_C(k,\ n) \quad (38)$$

$$d_{\alpha\beta_4}^{b_{IV}}=\frac{1}{2}(d_{\alpha\beta_1}-d_{\alpha\beta_2}-d_{\alpha\beta_3}+d_{\alpha\beta_4})$$
$$=\frac{1-(-1)^{l+j}-(-1)^{l+k}+(-1)^{j+k}}{2}u_A(i,\ l)\,u_B(j,\ m)\,u_C(k,\ n) \quad (39)$$

The domain of $(l,\ m,\ n)$ is the interior of the region made by the three boundary planes-which satisfies following conditions-including the halves of each planes: $l(1-N_B)+m(1-N_A)+N_A N_B>1$, $m(1-N_C)+n(1-N_B)+N_B N_C>1$, and $n(1-N_A)+l(1-N_C)+N_A N_C>1$.

Discussion

Depending on the atomic orbitals, the interactions (the reasonance integrals) could be identical each other. For instance, in the case of d_{xy} orbital it must hold by the symmetry that $t_{1x}=t_{1y}$ and $t_{2yz}=t_{2xz}$. Then Eq. (17) can be rewritten

$$\varepsilon_\beta=\varepsilon_0+2\left(t_{1x}\cos\frac{l\pi}{N_A+1}+t_{1x}\cos\frac{m\pi}{N_B+1}+t_{1z}\cos\frac{n\pi}{N_C+1}\right)$$
$$+4\left(t_{2xy}\cos\frac{l\pi}{N_A+1}\cos\frac{m\pi}{N_B+1}\right.$$
$$+t_{2yz}\cos\frac{m\pi}{N_B+1}\cos\frac{n\pi}{N_C+1}$$
$$\left.+t_{2xz}\cos\frac{n\pi}{N_C+1}\cos\frac{l\pi}{N_A+1}\right)$$
$$+8t_3\cos\frac{l\pi}{N_A+1}\cos\frac{m\pi}{N_B+1}\cos\frac{n\pi}{N_C+1} \quad (40)$$

Using Bloch sums, Slater and Koster[13] have derived the energy expression for infinite crystals, corresponding to above. Their expression, of course, has wave vecotr $\vec{k}=(k_x,\ k_y,\ k_z)$ as good quantum number. For d_{xy} orbital, Bloch sums are given by

$$\Psi_{d_{xy}}(\vec{k},\ \vec{r})=\sum_{\vec{R}_n}e^{i\vec{k}\cdot\vec{R}_n}d_{xy}(\vec{r}-\vec{R}_n) \quad (41)$$

and the energy expression is

$$\langle\Psi_{d_{xy}}(\vec{k},\ \vec{r})|\hat{H}|\Psi_{d_{xy}}(\vec{k},\ \vec{r})\rangle=E_{xy,\ xy}(0,\ 0,\ 0)$$
$$+2\{E_{xy,\ xy}(1,\ 0,\ 0)\ (\cos\xi+\cos\eta)+E_{xy,\ xy}(0,\ 0,\ 1)\ \cos\zeta\}$$
$$+4\{E_{xy,\ xy}(1,\ 1,\ 0)\ \cos\xi\cos\eta$$
$$+E_{xy,\ xy}(0,\ 1,\ 1)\ (\cos\xi\cos\zeta+\cos\eta\cos\zeta)\}$$
$$+8E_{xy,\ xy}(1,\ 1,\ 1)\ \cos\xi\cos\eta\cos\zeta \quad (42)$$

where $\xi=k_x a$, $\eta=k_y a$, and $\zeta=k_z a$, a being the unit cell dimension of the parent s.c. lattice. $E_{xy,\ xy}$ $(i,\ j,\ k)$ means an integral in which the functions φ_n are d_{xy}-like type orbitals and the direction cosines of the vector between atoms are $i,\ j$ and k. From Eq. (42), theenergy expressions of lattices, with only nearest neighbor interactions, can be written as

$$\langle\Psi_{d_{xy}}(\vec{k},\ \vec{r})|\hat{H}|\Psi_{d_{xy}}(\vec{k},\ \vec{r})\rangle=E_{xy,\ xy}(0,\ 0,\ 0)$$
$$+4\{E_{xy,\ xy}(1,\ 1,\ 0)\ \cos\xi\cos\eta$$
$$+E_{xy,\ xy}(0,\ 1,\ 1)\ (\cos\xi\cos\zeta+\cos\eta\cos\zeta)\} \quad (43)$$

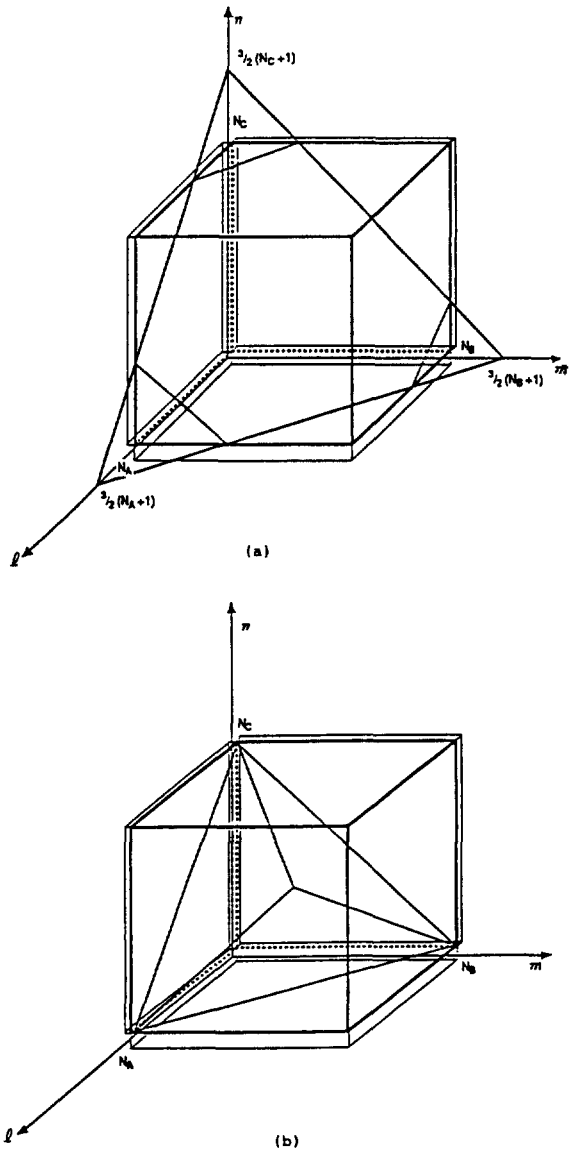

Figure 5. The domain of (l, m, n). (a) and (b) display the domains of f.c.c. and b.c.c. subclusters, respectively.

for f.c.c. lattice, and

$$\langle \Psi_{d_{xy}}(\vec{k}, \vec{r})|\hat{H}|\Psi_{d_{xy}}(\vec{k}, \vec{r})\rangle = E_{xy,\,xy}(0,\ 0,\ 0) + 8\,E_{xy,\,xy}(1,\ 1,\ 1)\ \cos\xi\cos\eta\cos\zeta \qquad (44)$$

for b.c.c. lattice. In Eq. (43) and (44), the wave vector $\vec{k}=(k_x, k_y, k_z)$ (consequently ξ, η and ζ) is limited to the Brillouin zone. In the case of the finite cluster, the vector (l, m, n) must be limited to a certain domain. The two-fold degenerate states originated from the two f.c.c. subclusters of this parent s.c. cluster must be located each other symmetrically with respect to the plane passing through the point $q_c=\left(\frac{N_A+1}{2}, \frac{N_B+1}{2}, \frac{N_C+1}{2}\right)$. Figure 5(a) shows the domain of the states of f.c.c. subclusters bounded by the plane $\frac{l}{N_A+1}+\frac{m}{N_B+1}+\frac{n}{N_C+1}=\frac{3}{2}$, which is a face of the Brillouin zone. And

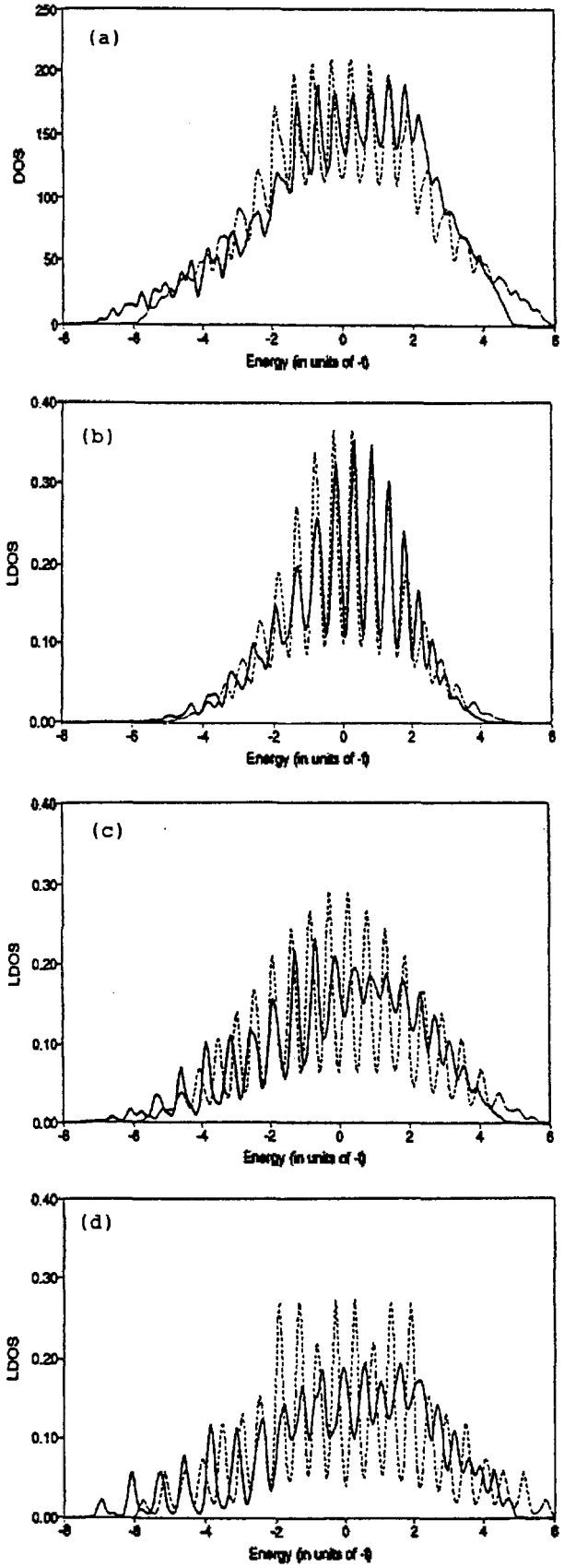

Figure 6. (a) DOS and LDOSs of 10×10×10 s.c. cluster at (b) (1, 1, 1), (c) (5, 5, 1) and (d) (5, 5, 5). The solid lines denote present work and the dashed lines correspond to Messmer's results.

one of the two obviously displays a part of the Brillouin zone, where each component of wave vector $\vec{k}$ is positive. In the case of b.c.c., the rectangular parallelepiped domain of states for the parent s.c. cluster must be divided into four, since the energy form described by Eq. (35) has four-fold degeneracy due to the four subclusters. Figure 5(b) displays the domain of staes for one of b.c.c. clusters in state-space, which is similar with the Brillouin zone of wave vector $\vec{k}$ of positive components. As the size of cluster becomes infinitely large, the domains merge into the Brillouin zone of positive directional wave vector $\vec{k}$ by which the energies of Eq. (43) and (44) are defined.

Using our analytical cluster solution, DOS and LDOS which sketch the distribution of states *vs.* energy, are computed. For a finite cluster, DOS and LDOS at α-atom can be defined by Gaussian function of width parameter σ[18]:

$$\rho^c(E)=(2\pi\sigma^2)^{-\frac{1}{2}}\sum_{\beta}\exp\left[-(E-\varepsilon_\beta)^2/2\sigma^2\right] \quad (45)$$

$$\rho_\alpha^c(E)=(2\pi\sigma^2)^{-\frac{1}{2}}\sum_{\beta}|d_{\alpha\beta}|^2\exp\left[-(E-\varepsilon_\beta)^2/2\sigma^2\right]. \quad (46)$$

In this work, $\varepsilon_0=0$ and $\sigma=0.1$ (in units of t) are assumed, and the clusters, which are the objects of our study, are cubic shape, and composed of about a thousand atoms. The size of these clusters is believed to be of that of a colloid used practically. Atomic *s*-orbital is chosen as a basis of clusters for simplicity. With this choice, the dependence of interaction on each directions is removed, since *s*-orbital is spherically symmetric. That is $t_{1x}=t_{1y}=t_{1z}=t_1$ and $t_{2xy}=t_{2yz}=t_{2xz}=t_2$ hold. Figure 6 shows DOS and LDOS of s.c. cluster. Messmer's results (dotted lines) are compared with our results (solid lines) in which interactions up to 3rd nearest neighbor are included, with the choice of $t=t_1=10t_2=100t_3$. The ratio is taken after the values usually used in extended Hückel calculation. Figure 7 and 8 are DOS and LDOS of f.c.c. and b.c.c. cluster, respectively, and they correspond to those of I-subcluster of Figure 3 and 4. The general profiles of LDOSs in all the considered lattices are similar to those of DOSs, but in detail, are fairly different each other. The shapes of LDOSs at vertex and surface of clusters are distinctive. The LDOSs near Fermi level, are larger at vertex and surface of clusters than inside the bulk. This means that the atomic orbitals at vertex and surface region are more contributive to MOs near the Fermi level (HOMO and LUMO) than those of inside. In s.c. cluster, considering only nearest neighbor interactions, one obtained the symmetric DOS and LDOS centered at the energy of isolated atom,[11] but with the introduction of 2nd nearest neighbor interactions, this symmetry is lost. Figure 7 shows that the DOS and LDOS of f.c.c. cluster are fairly unsymmetric. For the b.c.c. cluster, the DOS and LDOS are symmetric and unusually dense at center with comparison to other lattices. This means that the atomic orbitals are less perturbed in b.c.c. cluster than in others. This also implies that the Hückel method, with only the nearest neighbor interactions taken into account, is more coarse in b.c.c. than in other cluster. In fact, the ratio of 1st to 2nd nearest neighbor distance is 1.155 in b.c.c. lattices, but 1.414 in others.

In contrast with organic molecules, the lattice structures have 2nd nearest neighbors whose distance is not long

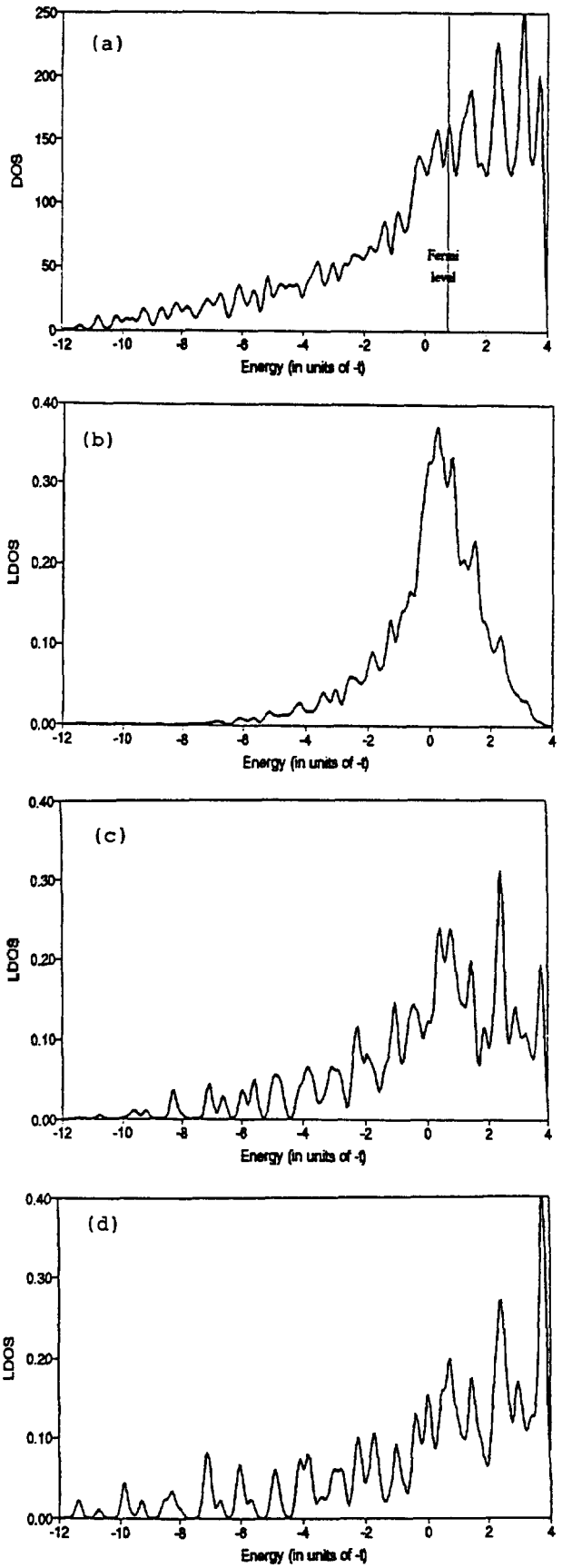

Figure 7. (a) DOS and LDOSs of f.c.c. I-cluster of 1014 atoms (of 13×13×12 parent s.c. cluster) at (b) (1, 1, 1), (c) (7, 7, 1) and (d) (7, 7, 5).

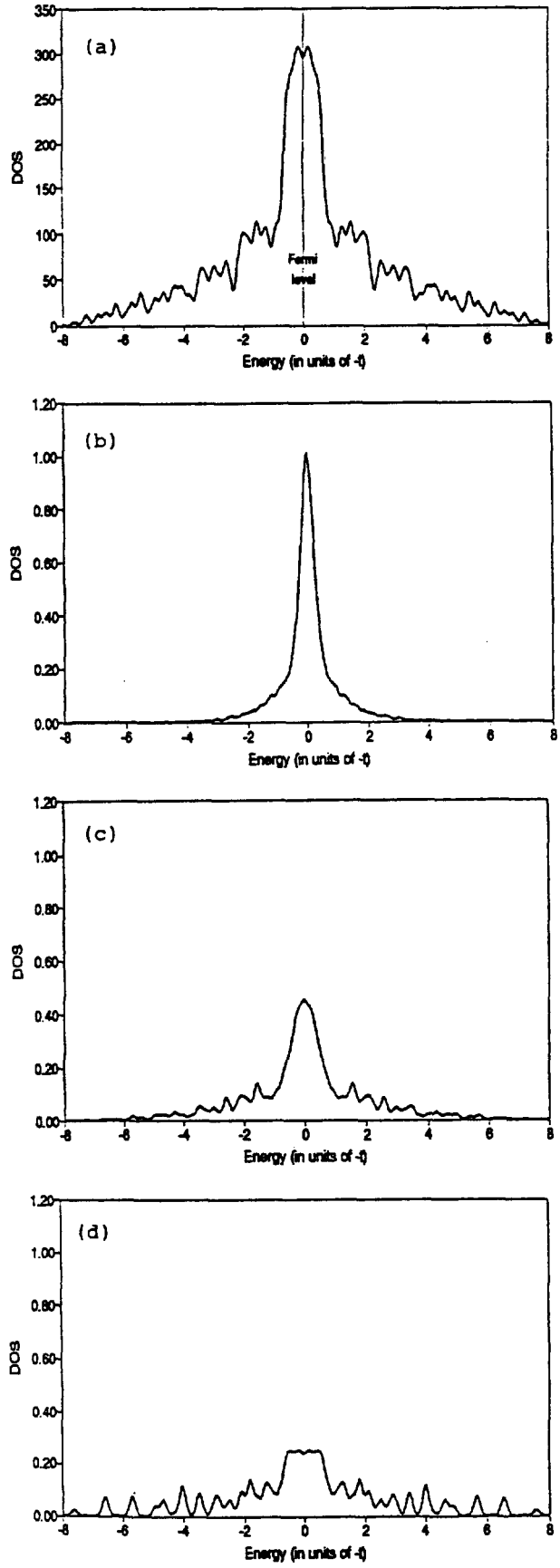

Figure 8. (a) DOS and LDOSs of b.c.c. I-cluster of 1024 atoms (of $16\times16\times16$ parent s.c. cluster) at (b) (1, 1, 1), (c) (7, 7, 1) and (d) (8, 8, 8).

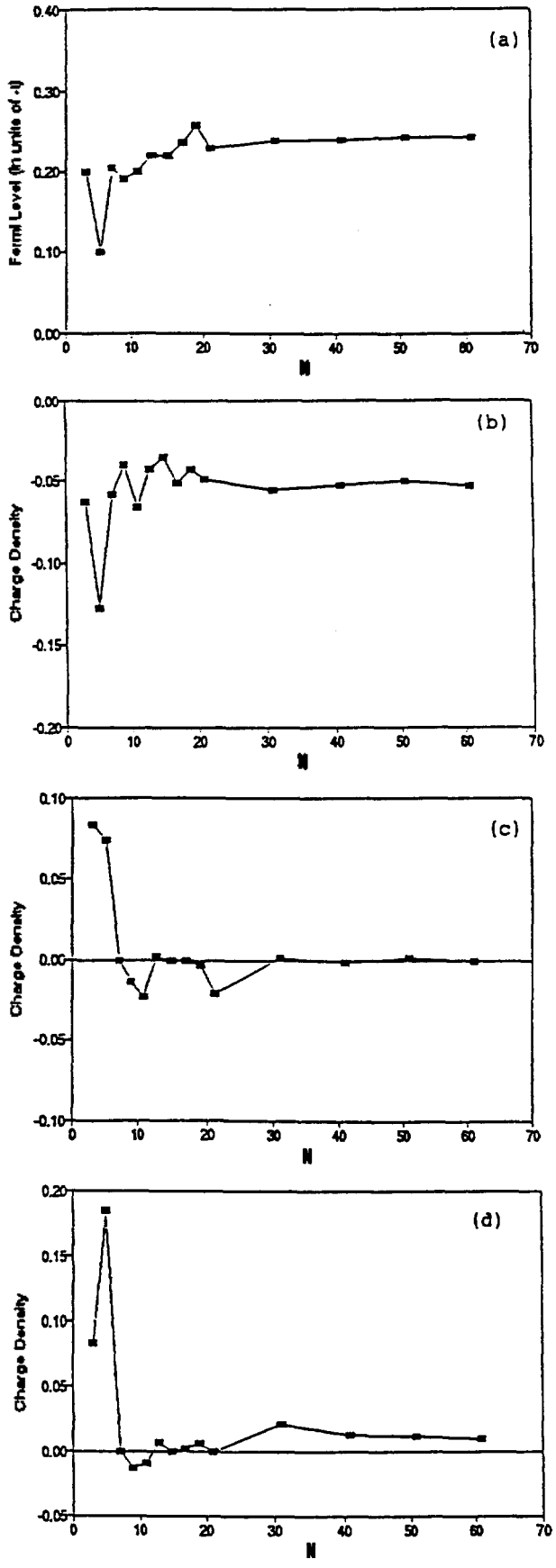

Figure 9. Plots of (a) Fermi level and charge densities of s.c. clusters at (b) vertex, (c) face, and (d) bulk center *vs.* the dimension of the cluster N. The size of clusters is $N\times N\times5$.

Table 1. Comparison of The Energies by Numerical Method with Those by Analytic One, in 5×4×3 Parent s.c. Cluster[a] (in units of-t)

s.c.[b]			Numerical	f.c.c.[c]			Numerical	b.c.c.[d]			Numerical
1st	Analytical upto 2nd	upto 3rd		1st	Analytical upto 2nd[e]	upto 2nd[f]		1st	Analytical upto 2nd[e]	upto 2nd[f]	
−4.76430	−5.51832	−5.55796	−5.55796	−7.54025	−7.70206	−7.79636	−7.79713	−3.96336	−4.61057	−4.98780	−5.00595
−4.03225	−4.56430	−4.58718	−4.58718								
−3.76430	−4.20370	−4.21884	−4.21884	−5.32049	−5.28230	−5.40994	−5.41104				
−3.35008	−3.63034	−3.63034	−3.63034								
−3.03225	−3.32288	−3.33162	−3.33162	−4.39399	−4.33219	−4.47121	−4.47222	−2.28825	−2.13546	−2.64602	−2.68935
−3.03225	−3.26107	−3.26107	−3.26107	−3.26107							
−2.61803	−2.77984	−2.77984	−2.77984	−2.90628	−2.76432	−2.90863	−2.90954				
−2.52823	−2.57873	−2.56359	−2.56359								
−2.35008	−2.45713	−2.45713	−2.45713	−2.80252	−2.64448	−2.81684	−2.81838	−1.51387	−1.26665	−1.82276	−1.86149
−2.03225	−2.11965	−2.11965	−2.11965								
−2.03225	−1.95785	−1.93496	−1.93496	−2.28825	−2.15005	−2.29436	−2.29552				
−1.93587	−1.78839	−1.77965	−1.77965								
−1.79618	−1.74235	−1.70272	−1.70272	−1.61803	−1.37984	−1.55748	−1.55908	−0.87403	0.15279	−0.51626	−0.61343
−1.61803	−1.67984	−1.67984	−1.67984								
−1.61803	−1.61803	−1.61803	−1.61803	−1.07047	−0.80866	−0.99796	−0.99922				
−1.52823	−1.26410	−1.22447	−1.22447								
−1.30020	−1.00697	−1.00697	−1.00697	−0.87403	−0.51223	−0.70126	−0.70341	0.00000	0.17318	−0.42444	−0.52927
−1.20382	−1.00382	−0.97250	−0.97250								
−1.11402	−0.99538	−0.96419	−0.96419	−0.61803	−0.44319	−0.58222	−0.58350				
−1.03225	−0.91643	−0.90769	−0.90769								
−0.93587	−0.71057	−0.70878	−0.70878	−0.50499	−0.15623	−0.37859	−0.38157	0.00000	0.55279	−0.02444	−0.26710
−0.79618	−0.70878	−0.69543	−0.69543								
−0.79618	−0.61803	−0.61803	−0.61803	0.00000	0.33820	0.14389	0.13328				
−0.61803	−0.54697	−0.52409	−0.52409								
−0.61803	−0.45623	−0.45623	−0.45623	0.00000	0.33966	0.16729	0.16378	0.00000	0.95279	0.24223	0.13033
−0.38197	−0.32016	−0.32016	−0.32016								
−0.30020	−0.03680	−0.02806	−0.02806	0.07785	0.56180	0.32278	0.33284				
−0.20382	−0.03560	−0.02047	−0.02047								
−0.20382	0.02500	0.02500	0.02500	0.61803	0.78220	0.65456	0.65175	0.0000	1.04721	0.29110	0.40000
−0.11402	0.16624	0.16624	0.16623								
0.11402	0.37084	0.36210	0.36210	0.74400	1.07984	0.85748	0.86031	0.0000	1.04721	0.29110	0.40000
0.20382	0.39427	0.39427	0.39427								
0.20382	0.43265	0.43265	0.43264	0.87403	1.23584	1.04681	1.04855				
0.30020	0.44377	0.44377	0.44377								
0.38197	0.56479	0.54965	0.54965	1.07047	1.33227	1.14324	1.14520	0.0000	1.44721	0.69110	0.56569
0.61803	0.61803	0.61803	0.61803								
0.61803	0.77984	0.77984	0.77984	1.15822	1.42002	1.24766	1.24789				
0.79618	0.88358	0.88358	0.88358								
0.79618	1.04539	1.02250	1.02250	1.61803	1.77341	1.67859	1.67483	0.00000	1.76108	0.95777	0.88297
0.93587	1.14807	1.13933	1.13933								
1.03225	1.16118	1.14604	1.14604	1.67021	1.85623	1.67911	1.68034				
1.11402	1.22106	1.22106	1.22106								
1.20382	1.41226	1.38938	1.38938	1.93522	1.93202	1.75965	1.76357	0.0000	1.84721	1.20497	1.24004
1.30020	1.55623	1.55623	1.55623								
1.52823	1.59657	1.55694	1.55694	2.08443	2.12262	1.99498	1.99195				
1.61803	1.61803	1.61803	1.61803								
1.61803	1.79236	1.75272	1.75272	2.25306	2.31486	2.17583	2.17347	0.87403	1.92125	1.23180	1.27193
1.79618	1.80397	1.79522	1.79522								
1.93587	1.94484	1.94484	1.94484	2.28825	2.42644	2.28214	2.27522				
2.03225	2.10665	2.08377	2.08377								
2.03225	2.12939	2.08976	2.08976	2.49207	2.47947	2.38516	2.38843	1.51387	2.23721	1.29110	1.36569
2.35009	2.24304	2.24304	2.24304								
2.25823	2.45623	2.45623	2.45623	2.64127	2.53026	2.40262	2.41049				
2.61803	2.47773	2.46259	2.46259								
3.03225	2.74162	2.75036	2.75036	2.64592	2.70773	2.56870	2.57213	2.28825	2.44103	1.93047	1.98074
3.03225	2.80342	2.80342	2.80342								
3.35009	3.06983	3.06983	3.06983	2.80252	2.80196	2.69641	2.69743				
3.76430	3.32490	3.34004	3.34004								
4.03225	3.50020	3.52308	3.52308	2.96376	2.84071	2.70765	2.71916	3.96336	3.31614	2.93892	2.95997
4.76430	4.01027	4.04991	4.04991								

[a] For f.c.c., the one subcluster of 30 atoms is considered, and the one subclusters of 16 atoms for b.c.c. [b] The interactions up to 3rd nearest neighbors, are counted. The ratios of $t_1/t_2/t_3$ is $-1/-0.1/-0.01$. [c] The interactions up to 2nd nearest neighbors, are taken into account. The ratios of t_1/t_2 is $-1/-0.1$ [d] The interactions up to 2nd nearest neighbors, are considered. The ratios of t_1/t_2 is $-1/-0.6$ [e] The results are based of ref. (13) [f] Present work.

enough to be ignored. Let's consider 4th nearest neighbor interactions in s.c. cluster (*i.e.*, 2nd nearest neighbor interactions in f.c.c. and b.c.c. clusters). When 4th nearest neighbor interaction is introduced, l, m and n are no longer good guantum number, and the states between different l's, m's and n's are mixed due to the effect of surface. Therefore, we may add the diagonal 4th nearest neighbor interactions evaluated with the analytic cluster function.

$$\varepsilon_\beta=\varepsilon_0+2\left(t_{1x}\cos\frac{l\pi}{N_A+1}+t_{1y}\cos\frac{m\pi}{N_B+1}+t_{1z}\cos\frac{n\pi}{N_C+1}\right)$$
$$+4\left(t_{2xy}\cos\frac{l\pi}{N_A+1}\cos\frac{m\pi}{N_B+1}\right.$$
$$+t_{2yz}\cos\frac{m\pi}{N_B+1}\cos\frac{n\pi}{N_C+1}$$
$$\left.+t_{2xz}\cos\frac{n\pi}{N_C+1}\cos\frac{l\pi}{N_A+1}\right)$$
$$+8t_3\cos\frac{l\pi}{N_A+1}\cos\frac{m\pi}{N_B+1}\cos\frac{n\pi}{N_C+1}$$
$$+2\left(t_{4x}\cos\frac{2l\pi}{N_A+1}+t_{4y}\cos\frac{2m\pi}{N_B+1}+t_{4z}\cos\frac{2n\pi}{N_C+1}\right)$$
$$+4\left(\frac{t_{4x}}{N_A+1}\sin^2\frac{l\pi}{N_A+1}+\frac{t_{4y}}{N_B+1}\sin^2\frac{m\pi}{N_B+1}\right.$$
$$\left.+\frac{t_{4z}}{N_C+1}\sin^2\frac{n\pi}{N_C+1}\right). \quad (47)$$

The 5th term of Eq. (47) is the expression corresponding to the nearest neighbor interactions in s.c. structure, but twice as far away. The last term, which does not have its analogue in infinite crystal, comes from the existence of surface in a finite cluster. Table 1 shows the corrections of the energies introduced with the additional interactions. It is assumed that the ratio of 1st to 2nd or 2nd to 3rd nearest neighbor interactions can be given by

$$\frac{H_{\mu\nu}(R')}{H_{\mu\nu}(R)}=\frac{S_{\mu\nu}(R')}{S_{\mu\nu}(R)}=\frac{e^{-R'}(1+R'+R'^2/3)}{e^{-R}(1+R+R^2/3)}. \quad (48)$$

To inspect the local charge density and Fermi level, it is assumed that there is one electron per each atomic s-orbital. The charge density at α-atom can be defined

$$\delta_\alpha=1-\sum_\mu n_\mu d_{\alpha\mu}^2 \quad (49)$$

where n_μ is the occupation number of μ-th MO. Figure 9 and 10 show the charge densities at representative sites and Fermi levels of s.c. cluster with the interactions up to 3rd nearest neighbors, and f.c.c. cluster with only the nearest neighbor interactions, respectively. These values converge as the size of cluster becomes larger. To the contrary to the expectation, It is found that these properties of the s.c. cluster with only nearest neighbor interactions and b.c.c. cluster do not have any difference with these free atoms. Therefore, the above mentioned features of s.c. cluster with the interactions up to 3rd nearest neighbor, seem to be originated solely from the interaction of f.c.c. network which is substructure of this cluster. And it is interesting to note that electron density becomes larger at surface than at center, and at vertex than at surface.

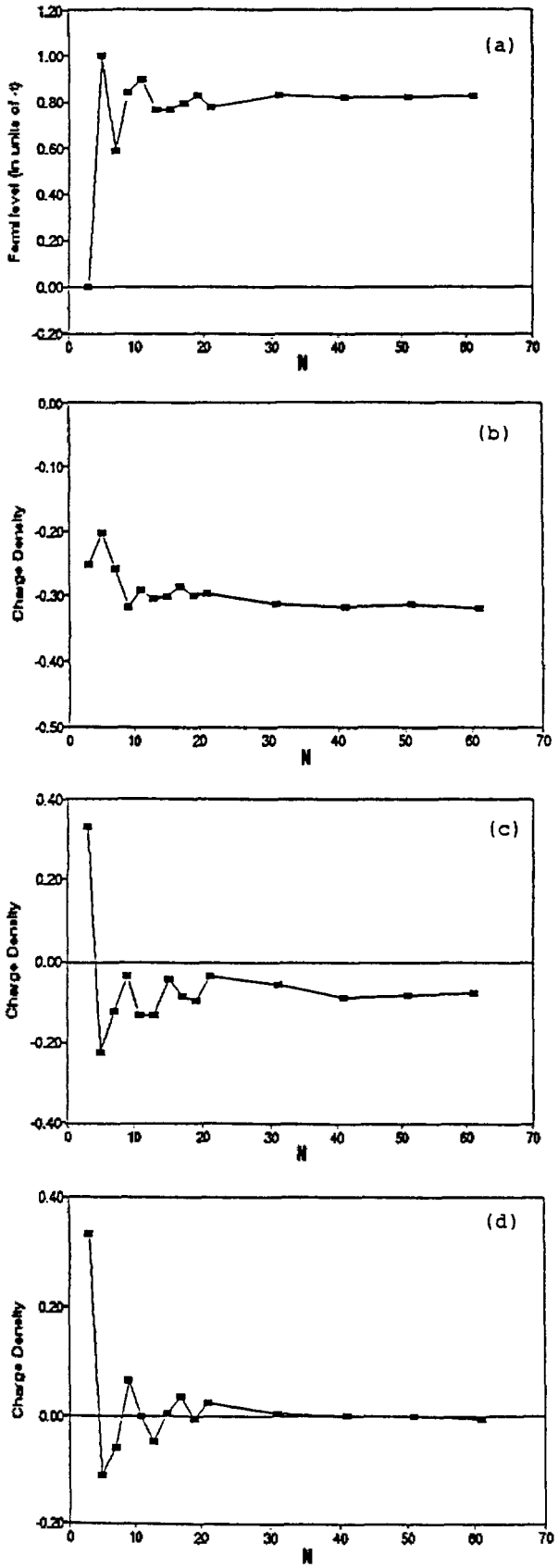

Figure 10. Plots of (a) Fermi level and charge densities of f.c.c. clusters at (b) vertex, (c) face, and (d) bulk center *vs.* N. The N is the edge length of the parent s.c. cluster ($N\times N\times 5$) from which th f.c.c. clusters is born out.

In the present treatment of the cluster orbitals, the major drawback is the limitation on the shape of a cluster. A cluster must be rectangular parallelepiped and have the surface characterized as (1, 0, 0)-plane.

Acknowledgement. This work has been supported by the Korea Science and Engineering Foundation.

References

1. A. W. Chan and R. Hoffmann, *J. Chem. Phys.*, **92**, 699 (1990).
2. A. T. Amos, P. A. Brook, and S. A. Moir, *J. Phys. Chem.*, **92**, 733 (1988).
3. C. Zheng, Y. Apeloig, and R. Hoffmann, *J. Am. Chem. Soc.*, **110**, 749 (1988).
4. H. Castejon, A. J. Hernandez, and F. Ruette, *J. Phys. Chem.*, **92**, 4970 (1988).
5. C. Calandra, F. Manghi, and C. M. Bertoni, *Surface Sci.*, **162**, 605 (1985).
6. H. Jörg and N. Rösch, *Surface Sci.*, **163**, L627 (1985).
7. Z. Tian, K. Zhang, and X. Xie, *Surface Sci.*, **163**, 1 (1985).
8. F. Illas, M. Bachs, and J. Rubio, *J. Chem. Phys.*, **91**, 5466 (1989).
9. J. Koutecky, U. Hanke, P. Fantucci, V. Bonacic-Koutecky, and D. Papierowska-Kaminski, *Surface Sci.*, **165**, 161 (1986).
10. M. Causa, R. Dovesi, C. Pisani, and C. Roetti, *Surface Sci.*, **175**, 551 (1986).
11. R. P. Messmer, *Phys. Rev.*, **B15**, 1811 (1977).
12. O. Bilek and P. Kadura, *Phys. Status Solidi*, **B85**, 225 (1978).
13. J. C. Slater and G. F. Koster, *Phys. Rev.*, **94**, 1498 (1954).
14. L. Salem, *J. Phys. Chem.*, **89**, 5576 (1985).
15. C. Minot, A. Sevin, C. Leforestier, and L. Salem *J. Phys. Chem.*, **92**, 904 (1988).
16. G. H. Ryu and H. Kim, *Bull. Korean Chem. Soc.*, **12**, 39 (1991).
17. R. T. Gregory and D. L. Karny, "A Collection of Matrices for Testing Computational Algorithms", Wiley-Interscience, p. 137 (1969).
18. R. P. Messmer, in "The Nature of the Surface Chemical Bond", North-Holland Amsterdam, pp. 60-63 (1979).

Comparison of Photophysical and Photochemical Properties of Khellin and 8-Methoxypsoralen

Ho Kwon Kang*, Eun Ju Shin† and Sang Chul Shim‡

Department of Agricultural Chemistry, Sunchon National University, Sunchon 540-100
†Department of Chemistry, Sunchon National University, Sunchon 540-100
‡Department of Chemistry, Korea Advanced Institute of Science and Technology, Seoul 130-012.
Received May 27, 1991

The photophysical and photochemical properties of khellin were compared with those of 8-methoxypsoralen (8-MOP). Quantum yields of fluorescence and triplet formation decreases as solvent polarity increases, which is opposite to 8-MOP, and photocycloadditivity of khellin to olefins is much lower than that of 8-MOP. Electron ejection from khellin by laser flash was not observed, but observed from 8-MOP. As models of 4',5'-monoadducts of khellin or 8-MOP with thymine base, khellin<>dimethylfumarate 4',5'-monoadduct (KDF) was also compared with 8-MOP< >thymidine 4',5'-monoadduct (F-2) in those properties to give some insight on the second-step biadduct formation resulting in cross-links of DNA duplex. KDF ad F-2 were very similar to khellin and 8-MOP in photophysical properties, respectively. However, KDF did not form adducts with various olefins, and thus it is thought that 2,3-double bond of chromone moiety in khellin is hardly reactive in contrast with 3, 4-double bond of coumarin moiety in 8-MOP. These results indicate that khellin is fairly photostable compound, a poor type I photodynamic sensitizer and producer of O_2^- which is some cause of phototoxic erythemal reactions and undesirable side effects. Therefore khellin is safer to use than 8-MOP in photochemotherapy of some skin diseases. Although khellin is much less reactive than 8-MOP, khellin must be also a monofunctional drug. Since khellin is, however, as effective as 8-MOP in photochemotherapy of some skin diseases, it is suggested that khellin may be different from 8-MOP in the action mechanism.

Introduction

Furocoumarins are well-known skin photosensitizing agent and have been used in the treatment of various skin diseases such as *vitiligo*[1] and *psoriasis*[2] and as molecular probes for studying nucleic acid structure[3] and also more recently in the treatment of AIDS.[4] The biological effects of furocoumarins plus UV treatment appear to the mediated primarily by the formation of [2+2]-cyclobutane adducts which arise from [2+2]-photocycloaddition of the 3,4- and/or 4',5'-double bonds of furocomarin intercalated into duplex nucleic acid with the 5, 6-double bond of pyrimidine bases.[5] However,

*Author to whom correspndence should be addressed.